

the images that were created to simulations, in order to extract physics from them. The doughnut is real — it exists.

Professor Mike Edmunds. You were telling us about the Blandford chemical model with $1/r$ and $1/r^2$ for tangential and parallel components. If you have an accelerating flow what would it do? Presumably people have modelled it since 1977?

Dr. Röder. That is true but I couldn't say off the top of my head.

Professor Edmunds. We can work it out. If the thing is accelerating then you are going to lower densities essentially; does the magnetic field just go with the density?

Dr. Röder. I would assume that it is not necessarily tied to the particle number density; if everything stretches out then it will also dissipate faster, I would guess.

Professor Edmunds. I'm just surprised that there isn't a modelling that has done that.

The Senior Secretary. Are there any other questions? Thank you very much again for an excellent talk [applause]. It just leaves me to give notice that the next A & G Highlights meeting of the Society will be Friday, November 8th at 4 pm and I believe it will be here. Finally there is a small drinks reception in the Council Room immediately after we finish and you are all welcome to attend. Thanks very much again to all our speakers and questioners.

REDISCUSSION OF ECLIPSING BINARIES. PAPER 23:
THE F-TYPE TWIN SYSTEM RZ CHAMAELEONTIS

By John Southworth

Astrophysics Group, Keele University

RZ Cha is a detached eclipsing binary containing two slightly evolved F5 stars in a circular orbit of period 2.832 d. We use new light-curves from the *Transiting Exoplanet Survey Satellite* (*TESS*) and spectroscopic orbits from *Gaia* DR3 to measure the physical properties of the component stars. We obtain masses of $1.488 \pm 0.011 M_{\odot}$ and $1.482 \pm 0.011 M_{\odot}$, and radii of $2.150 \pm 0.006 R_{\odot}$ and $2.271 \pm 0.006 R_{\odot}$. An orbital ephemeris from the *TESS* data does not match published times of mid-eclipse from the 1970s, suggesting the period is not constant. We measure a distance to the system of 176.7 ± 3.7 pc, which agrees with the *Gaia* DR3 value. A comparison with theoretical models finds agreement for metal abundances of $Z = 0.014$ and $Z = 0.017$ and an age of 2.3 Gyr. No evidence for pulsations was found in the light-curves. Future data from *TESS* and *Gaia* will provide more precise masses and constraints on any changes in orbital period.

Introduction

The current series of papers¹ is concerned with determining the physical properties of detached eclipsing binary systems (dEBs) to sufficient precision to be useful for testing the predictions of theoretical stellar models. The intended precision is 2% or better in the masses and radii of the component stars^{2,3}, although precisions in the region of 0.2% can be achieved in the best cases⁴. Our work uses published spectroscopic radial-velocity (RV) measurements combined with new photometry from space missions such as *Kepler*⁵ and *TESS*⁶, which have revolutionized our understanding of binary stars⁷.

In this work we turn our attention to the system RZ Chamaeleontis (Table I), a partially-eclipsing dEB containing two almost identical F-stars on a circular orbit of period 2.828 d. Its variability was discovered by Strohmeier, Knigge & Ott⁸ under the moniker of BV 473, from Bamberg photographic patrol plates. Popper⁹ obtained nine photographic spectra and commented that there were lines of two components with approximately equal intensity. Geyer & Knigge¹⁰ refined the period to 2.832093(61) d from *UBV* observations of most of one eclipse.

Jørgensen & Gyldenkerne¹¹ presented extensive photometry of RZ Cha obtained with the Copenhagen 50-cm telescope sited at ESO La Silla, Chile. They used the Strömgren photometer to obtain simultaneous observations in the *uvby* passbands, totalling 775 points in each band. They fitted the light-curves using a rectification procedure^{12,13}, finding the ratio of the radii (k) to be close to unity but poorly determined due to the eclipses being partial. They thus fixed $k = 1$ to present results for the mean component of the system. The Strömgren colour indices were found to be practically the same for the two stars, supporting the imposition of $k = 1$ on the light-curve solution, and to indicate that they have an approximately solar metallicity ($[\text{Fe}/\text{H}] = -0.02 \pm 0.15$). They also found an effective temperature of $T_{\text{eff}} = 6580 \pm 150$ K for the two stars, and that they had evolved beyond the end of the main sequence.

In an accompanying paper, Andersen *et al.*¹⁴ (hereafter AGI75) presented photographic spectroscopic observations of RZ Cha from which the masses and radii of the mean component were deduced to 1–2% precision. A modest

TABLE I

Basic information on RZ Chamaeleontis. The BV magnitudes are each the mean of 129 individual measurements¹⁸ distributed approximately randomly in orbital phase. The \mathcal{JHK} magnitudes are from 2MASS¹⁹ and were obtained at an orbital phase 0.30.

| Property | Value | Reference |
|---------------------------------------|---|-----------|
| Right ascension (J2000) | 10 ^h 42 ^m 24 ^s .11 | 20 |
| Declination (J2000) | −82°02′14″.2 | 20 |
| Henry Draper designation | HD 93486 | 21 |
| <i>Gaia</i> DR3 designation | 5198334162577657984 | 22 |
| <i>Gaia</i> DR3 parallax | 5.7404 ± 0.0186 mas | 22 |
| <i>TESS</i> Input Catalog designation | TIC 394730113 | 23 |
| <i>B</i> magnitude | 8.54 ± 0.02 | 18 |
| <i>V</i> magnitude | 8.09 ± 0.01 | 18 |
| \mathcal{J} magnitude | 7.131 ± 0.030 | 19 |
| <i>H</i> magnitude | 6.941 ± 0.036 | 19 |
| <i>K_s</i> magnitude | 6.904 ± 0.038 | 19 |
| Spectral type | F5 IV–V + F5 IV–V | 14 |

disagreement was found between the two sets of photographic plates obtained, with the F-series (reciprocal dispersion 20 \AA mm^{-1}) yielding slightly smaller and more uncertain velocity amplitudes than the G-series (12.3 \AA mm^{-1}) plates. AGI75 found the two stars to be almost identical, with a magnitude difference between the spectral-line strengths of the components of $0.02 \pm 0.02 \text{ mag}$ (mean error from five spectral lines).

Giuricin *et al.*¹⁵ reanalysed the *wby* light-curves using the WINK program¹⁶, finding that they could differentiate between the two stars. Their results point towards one star being slightly hotter (by 50 K) and also slightly smaller (with $k = 1.061 \pm 0.020$ where the error bar neglects some sources of uncertainty such as limb darkening). This is plausible in a system where both components are evolved far from the zero-age main sequence. Giuricin *et al.* modelled the four light-curves separately and obtained very different results for the *y* band *versus* the others (for example, a ratio of the radii of 1.40 instead of 1.06), but did not even comment on this discrepancy. The small but detectable difference between the stars was restated by Graczyk *et al.*¹⁷, who included RZ Cha in a sample of 35 dEBs constructed to calibrate relations between surface brightness and colour.

Photometric observations

RZ Cha has been observed in seven sectors by the NASA *Transiting Exoplanet Survey Satellite*^{6,24} (*TESS*), at a variety of sampling rates. The data from sectors 11, 12, and 13 were obtained at a cadence of 1800 s, from sectors 38 and 39 at 600-s cadence, and from sectors 65 and 66 at both 120-s and 200-s cadence. An eighth set of observations is scheduled in the near future: sector 93 will be observed in 2025 June. In this work we concentrate on the data obtained at the highest available cadence.

We downloaded data for all sectors from the NASA Mikulski Archive for Space Telescopes (MAST*) using the LIGHTKURVE package²⁵. We specified the quality flag “hard” to retain only the best data, and used the simple aperture photometry (SAP) light-curves from the SPOC data-reduction pipeline²⁶. The data points were converted into differential magnitudes and the median magnitude was subtracted from each sector to normalize the data.

We show the resulting light-curves in Fig. 1. The temporal coverage in the final two sectors, on which we concentrate our efforts, is excellent. A total of 19 515 and 18 604 data points are available in sectors 65 and 66, respectively.

We queried the *Gaia* DR3 database[†] for all sources within 2 arcmin of RZ Cha. All of the 92 sources returned as a response to our query are fainter than RZ Cha by at least 5.01 mag in the *Gaia* G_{RP} passband. We therefore expect the amount of light contaminating the light-curve to be negligible. As a confirmation of this, the TICv8 catalogue²³ indicates that less than 1% of the light in the *TESS* light-curve of RZ Cha may be ascribed to contamination from nearby point sources.

Light-curve analysis

We combined together the 120-s cadence data of RZ Cha from *TESS* sectors 65 and 66 for a detailed analysis of the photometric variations due to binarity. The primary and secondary eclipses are of similar depth (approximately 0.4 mag)

*<https://mast.stsci.edu/portal/Mashup/Clients/Mast/Portal.html>

†<https://vizier.cds.unistra.fr/viz-bin/VizieR-3?-source=I/355/gaiadr3>

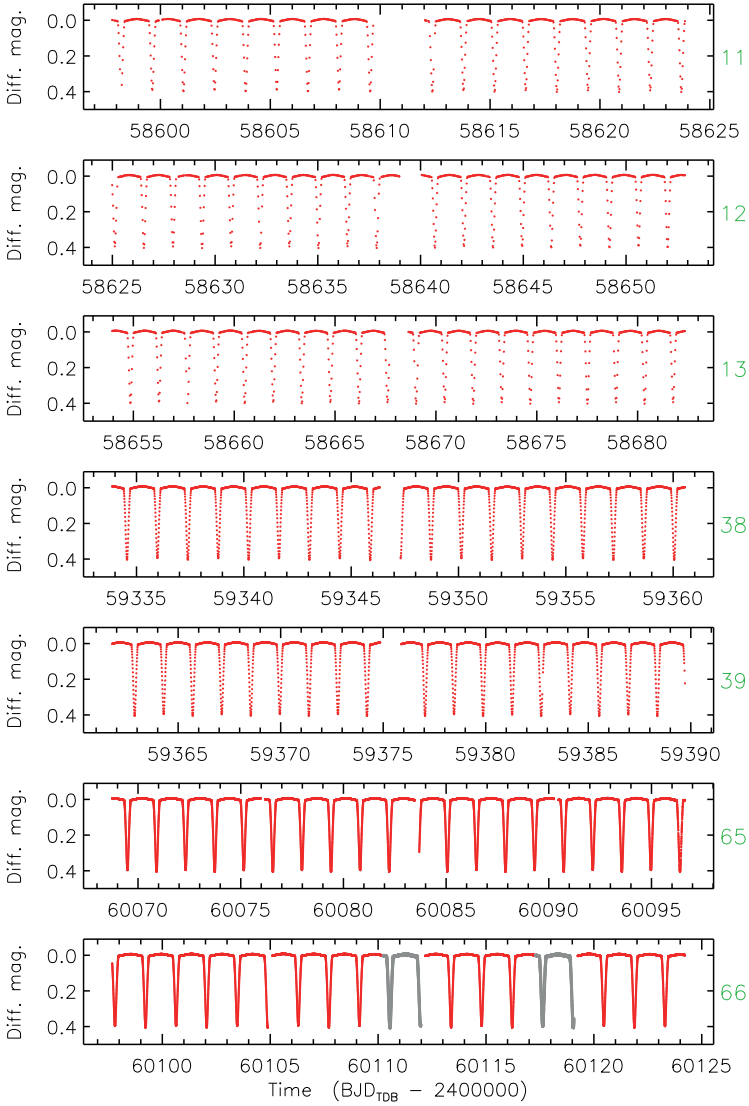


FIG. 1

TESS short-cadence SAP photometry of RZ Cha. The flux measurements have been converted to magnitude units then rectified to zero magnitude by subtraction of the median. Rejected observations are shown as grey open circles. The sector number is shown in green to the right of each panel.

but a difference in depth is apparent on visual inspection. We assigned a time of primary minimum close to the midpoint of the light-curve as our reference time of primary minimum (T_0) and define star A to be the star eclipsed at that time. Star A is therefore hotter than its companion, star B; it is also the smaller of the two. Their masses are not significantly different (see below).

We modelled the light-curve using version 43 of the JKTEBOP* code^{27,28}, fitting for the fractional radii of the stars (r_A and r_B), expressed as their sum ($r_A + r_B$) and ratio ($k = r_B/r_A$), the central-surface-brightness ratio (\mathcal{F}), third light (\mathcal{L}_3), orbital inclination (i), orbital period (P), and the reference time of primary minimum (T_0). Limb-darkening (LD) was included in the fit using the power-2 law^{29–31}, with the same coefficients used for both stars due to their strong similarity. The linear coefficient (c) was fitted and the non-linear coefficient (α) was fixed to a suitable theoretical value^{32,33}.

After some experimentation it became clear that there were two time intervals where the data had a significantly larger scatter. The affected data points were culled from the analysis and are shown in a different colour in Fig. 1. It was also apparent that there were slight discontinuities in flux associated with three gaps in the data for each of the two sectors. We therefore applied a total of eight quadratic functions to normalize the out-of-eclipse brightness of the system — four for each *TESS* sector. Once these adjustments were made we obtained an excellent fit to the *TESS* observations (Fig. 2). Our results consistently indicate that star A is hotter but smaller than star B.

To obtain error bars for the fitted parameters we decreased the size of the data errors from the *TESS* data-reduction pipeline to force a reduced χ^2 of unity, then ran the Monte-Carlo and residual-permutation simulations implemented in JKTEBOP^{27,34}. The measured parameter values and their error bars are given in Table II, and in all cases correspond to the residual-permutation values as they are larger than the Monte-Carlo error bars.

TABLE II

Photometric parameters of RZ Cha measured using JKTEBOP from the light-curves from TESS sectors 65 and 66. The error bars are 1σ and were obtained from a residual-permutation analysis.

| Parameter | Value |
|--------------------------------------|-------------------------------|
| <i>Fitted parameters:</i> | |
| Orbital period (d) | 2.8320896 ± 0.0000013 |
| Reference time (BJD _{TDB}) | $2460096.389351 \pm 0.000012$ |
| Orbital inclination ($^\circ$) | 83.2920 ± 0.0060 |
| Sum of the fractional radii | 0.36509 ± 0.00012 |
| Ratio of the radii | 1.0562 ± 0.0025 |
| Central-surface-brightness ratio | 0.98075 ± 0.00008 |
| Third light | 0.01641 ± 0.00075 |
| LD coefficient c | 0.5901 ± 0.0063 |
| LD coefficient α | 0.4898 (fixed) |
| <i>Derived parameters:</i> | |
| Fractional radius of star A | 0.17755 ± 0.00023 |
| Fractional radius of star B | 0.18753 ± 0.00019 |
| Light ratio ℓ_B/ℓ_A | 1.0972 ± 0.0052 |

*<http://www.astro.keele.ac.uk/jkt/codes/jktebop.html>

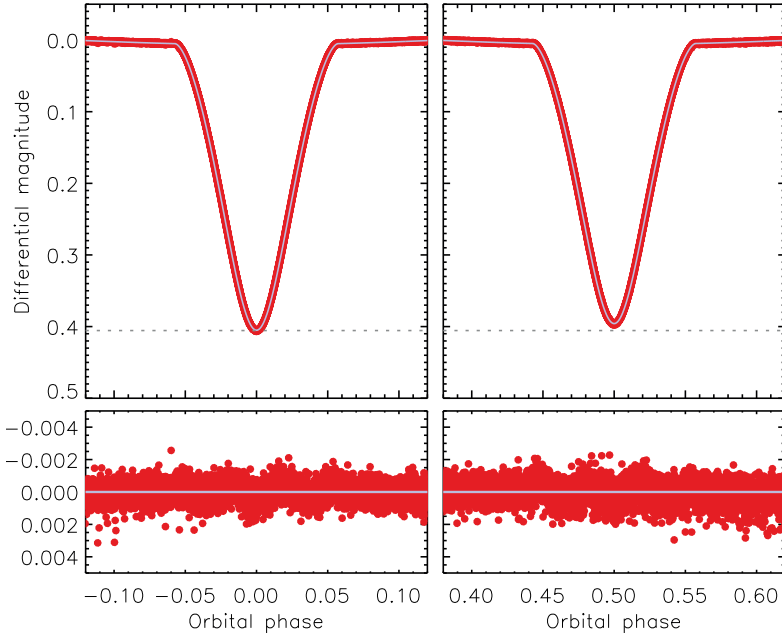


FIG. 2

JKTEBOP best fit to the 120-s cadence light-curves of RZ Cha from *TESS* sectors 65 and 66. The data are shown as filled red circles and the best fit as a light-blue solid line. A dotted line shows the brightness of the system at the midpoint of primary eclipse, and is a visual indicator of the slight difference in depths between the two eclipses. The residuals are shown on an enlarged scale in the lower panel.

Our results are in good agreement with previous analyses^{11,15} but with much smaller error bars. However, our light ratio is slightly inconsistent with the one given by AGI75 from their photographic spectra; the level of disagreement is ambiguous because AGI75 did not specify which star was which in the evaluation of their light ratio.

Orbital ephemeris

The analysis so far has used only two consecutive sectors of *TESS* observations, so P and T_0 are not as precise as they could be. We therefore fitted each of the *TESS* sectors individually using JKTEBOP to determine times of eclipse. We chose the primary eclipse closest to the midpoint of each sector as best representative of the full sector. We did not obtain any times of secondary eclipse, or times of individual eclipses, as this exceeds the scope of the current work. The times of minimum light used are given in Table III.

The orbital ephemeris from the six times of minimum light is

$$\text{Min I} = \text{BJD}_{\text{TDB}} 2459374.206471(3) + 2.832089764(13)E \quad (1)$$

and the residuals *versus* the best fit are plotted in Fig. 3. The times are measured

TABLE III

Times of primary eclipse for RZ Cha and their residuals versus the fitted ephemeris.

| Orbital cycle | Eclipse time (BJD _{TDB}) | Uncertainty (d) | Residual (d) |
|---------------|------------------------------------|-----------------|--------------|
| -260.0 | 2458637.863128 | 0.000012 | -0.000004 |
| -250.0 | 2458666.184023 | 0.000009 | -0.000007 |
| -10.0 | 2459345.885586 | 0.000008 | 0.000013 |
| 0.0 | 2459374.206474 | 0.000010 | 0.000003 |
| 250.0 | 2460082.228909 | 0.000007 | -0.000003 |
| 260.0 | 2460110.549807 | 0.000007 | -0.000003 |

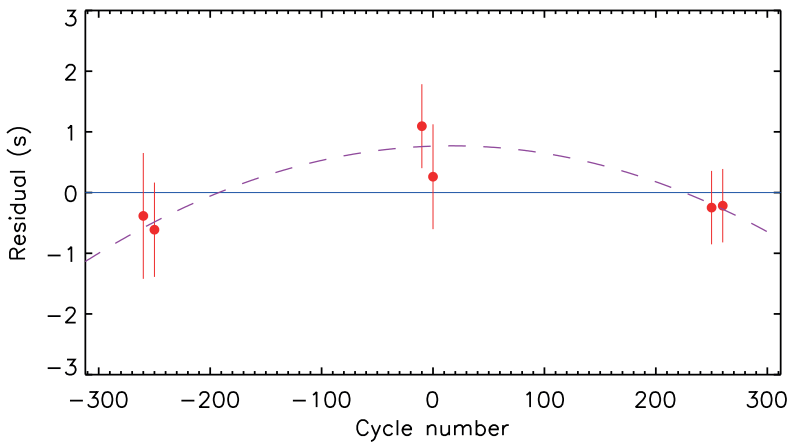


FIG. 3

Residuals of the times of minimum light from Table III (red circles) versus the best-fitting ephemerides. The blue solid line and purple dashed line indicate residuals of zero for the linear and quadratic ephemeris, respectively. Note the extremely small scale on the y -axis.

to an extraordinary precision, with a root-mean-square (rms) residual of only 0.56 s.

We then tried to project the orbital ephemeris back to the times of eclipse given by Jørgensen & Gyldenkerne¹¹, including also the time of minimum given by Mallama³⁵. This was unsuccessful because the gap of almost exactly 46 years between our timings and that of Mallama means we cannot confidently assign orbital cycle counts to the older data. We therefore rely on the ephemeris above, which is valid for the duration of the *TESS* data only.

RZ Cha may exhibit low-amplitude period variations. There is a hint of this in our own timings (Table III), where the addition of a quadratic term to the ephemeris lowers the r.m.s. of the residuals from 0.56 s to 0.27 s (Fig. 3), and it would also explain our difficulty in adding historical times of minimum to the analysis. Further support for this notion comes from a plot of the residuals versus an orbital ephemeris of RZ Cha on the TIDAK website^{*36}. We leave this matter to the future, where additional insight is expected from the extra sector of data from *TESS* as well as more extensive compilations of published times of minimum.

*<https://www.as.up.krakow.pl/minicalc/CHARZ.HTM>

Radial-velocity analysis

It is important to check the results of the RV analysis presented by AGI75 to ensure consistency with the numbers in the current work. AGI75 noticed an inconsistency between their results from the two series of photographic plates they used, the 20 \AA mm^{-1} plates giving slightly lower velocity amplitudes (K_A and K_B) than the 12 \AA mm^{-1} plates. The differences between measurements of the same plates by the various co-authors of the paper using their own methods* are smaller than both the inconsistency and the uncertainties. We have collected the various values of K_A and K_B in Table IV.

TABLE IV

Velocity amplitudes measured in different ways for RZ Cha. The person who performed the analysis is given in parentheses in each case.

| Source | K_A (km s^{-1}) | K_B (km s^{-1}) |
|---|------------------------------|------------------------------|
| 20 \AA mm^{-1} plates (Imbert) | 105.3 ± 2.7 | 103.6 ± 1.7 |
| 20 \AA mm^{-1} plates (Andersen) | 106.4 ± 0.8 | 106.5 ± 1.0 |
| 12 \AA mm^{-1} plates (Gjerløff) | 108.5 ± 0.6 | 108.7 ± 0.9 |
| 12 \AA mm^{-1} plates (Andersen) | 108.4 ± 0.7 | 107.0 ± 0.9 |
| AGI75 adopted value | 108.2 ± 0.6 | 107.6 ± 0.9 |
| 20 \AA mm^{-1} plates (this work) | 106.2 ± 1.3 | 105.5 ± 1.0 |
| 12 \AA mm^{-1} plates (this work) | 108.5 ± 0.6 | 107.8 ± 0.8 |
| 20 \AA mm^{-1} and 12 \AA mm^{-1} (this work) | 108.0 ± 0.6 | 106.7 ± 0.7 |
| <i>Gaia</i> DR3 tbosb2 | 107.8 ± 0.4 | 108.2 ± 0.4 |

We also extracted the RVs from table 1 of AGI75 to perform our own fits. It is not stated which co-author produced the tabulated RVs, but it is likely to have been Johannes Andersen as he was the only author to analyse both sets of photographic plates. As fitted parameters we specified K_A , K_B , the systemic velocity (assumed to be the same for both stars), and a phase offset with respect to our ephemeris in Table II. Uncertainties were calculated using Monte Carlo simulations, and the velocity amplitudes we found are given in Table IV.

Our first conclusion is that the phase offset is small, hence the primary star adopted by AGI75 is probably the same as our star A. This conclusion is valid only if changes in the orbital period in the system are small. We fitted the 20 \AA mm^{-1} RVs, finding an r.m.s. scatter of 3.2 km s^{-1} for star A and 2.5 km s^{-1} for star B. We then fitted the 12 \AA mm^{-1} RVs, obtaining scatters of 2.1 km s^{-1} and 3.4 km s^{-1} respectively. With these r.m.s. scatters applied as error bars to the RVs, we then fitted all the AGI75 RVs together (see Fig. 4). The systemic velocities in these fits were all in good agreement, so need not be discussed further.

RZ Cha has also been observed spectroscopically using the *RVS* instrument³⁷ on the *Gaia* mission, and the parameters of its spectroscopic orbit are given in the tbosb2 catalogue³⁸. Fifteen RVs were automatically measured and fitted for each star; the orbit has the correct period and a very small and negligible³⁹ eccentricity. We verified that the primary star in tbosb2 corresponds to our star A. The velocity amplitudes from tbosb2 are given in Table IV, are consistent with previous determinations, and have a smaller error bar. It is also clear that K_A is smaller and K_B is larger than previously found, to the extent that $K_B > K_A$.

*This author confesses he is far too young to have ever used a Grant comparator, although he vaguely remembers seeing one in a store-room at an observatory somewhere.

[†]<https://vizier.cds.unistra.fr/viz-bin/VizieR-3?-source=I/357/tbosb2>

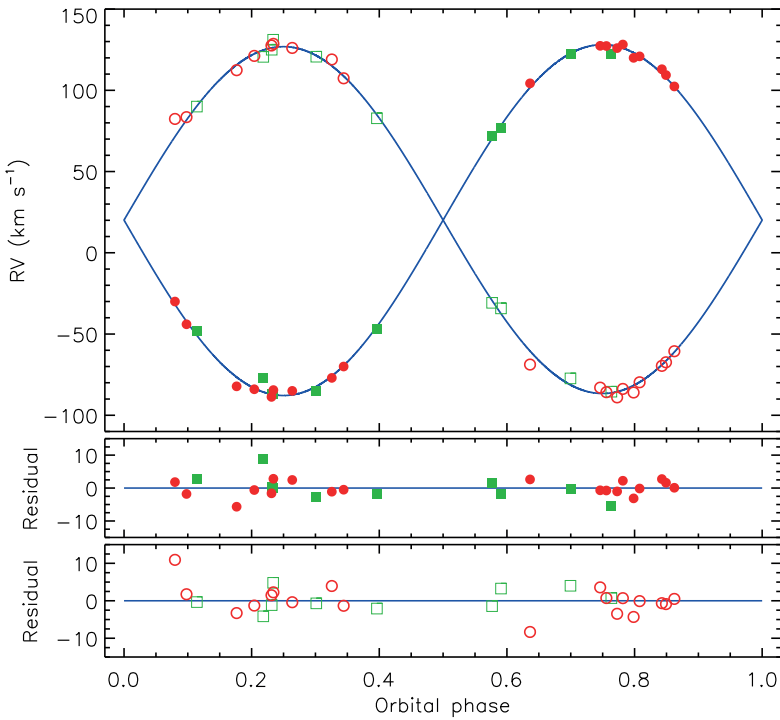


FIG. 4

RVs of RZ Cha from AGI75 compared to the best fit from JKTEBOP (solid-blue lines). The RVs for star A are shown with red filled circles for the 20 \AA mm^{-1} photographic plates and green filled squares for the 12 \AA mm^{-1} plates. The RVs for star B are shown with red open circles for the 20 \AA mm^{-1} photographic plates and green open squares for the 12 \AA mm^{-1} plates. The residuals are given in the lower panels separately for the two components.

We are thus faced with a choice between adopting the results based on the RVs of AGI75, which are derived from photographic observations and show some inconsistencies, or the orbit given in the tbsb2 catalogue based on RVs which are not public and thus cannot be verified. Issues with the tbsb2 orbits have previously been noted^{40–44}, but in the case of RZ Cha the orbital parameters are close to the values known from other sources. We have therefore decided to adopt the K_A and K_B from tbsb2, and note that this can be checked in the near future (late 2026) when *Gaia* DR4 becomes available*.

Physical properties and distance to RZ Cha

The physical properties of RZ Cha were determined using the JKTEBOP code⁴⁶ and the results from the analyses described above. The masses are measured to a precision of 0.7%, are not significantly different from each other,

* <https://www.cosmos.esa.int/web/Gaia/release>

and may be improved once *Gaia* DR4 is published. The radii are measured to a precision of 0.3%, and star B is larger and more evolved than star A. The masses and radii agree well with previous measurements^{11,14,15}, but are significantly more precise. There is an apparent inconsistency in that the less-massive star B is more evolved than its companion, but the significance of this is too low to be concerning: the mass ratio is only 0.8 σ below unity.

We adopted a T_{eff} of the system of 6580 ± 150 K¹¹ and used the surface-brightness ratio and equations from Southworth⁴⁷ to convert this to individual T_{eff} values (Table V). These T_{eff} values were used with the surface-brightness calibrations by Kervella *et al.*⁴⁸ and the apparent magnitudes in Table I to determine the distance to the system. A small amount of interstellar reddening of $E(B-V) = 0.05 \pm 0.02$ mag was needed to align the distances from the optical and infrared passbands. Our best distance estimate is 176.7 ± 3.7 pc in the K_s -band, which is in agreement with the 174.2 ± 0.6 pc from the *Gaia* DR3 parallax.

TABLE V

Physical properties of RZ Cha defined using the nominal solar units given by IAU 2015 Resolution B3 (ref. 45).

| Parameter | Star A | Star B |
|---|---------------------|---------------------|
| Mass ratio M_B/M_A | 0.9963 ± 0.0047 | |
| Semi-major axis of relative orbit (R_\odot^N) | 12.109 ± 0.029 | |
| Mass (M_\odot^N) | 1.488 ± 0.011 | 1.482 ± 0.011 |
| Radius (R_\odot^N) | 2.1499 ± 0.0058 | 2.2708 ± 0.0058 |
| Surface gravity (log[cgs]) | 3.9458 ± 0.0018 | 3.8967 ± 0.0017 |
| Density (ρ_\odot) | 0.1497 ± 0.0007 | 0.1266 ± 0.0005 |
| Synchronous rotational velocity (km s ⁻¹) | 38.41 ± 0.10 | 40.57 ± 0.10 |
| Effective temperature (K) | 6596 ± 150 | 6564 ± 150 |
| Luminosity log(L/L_\odot^N) | 0.897 ± 0.040 | 0.936 ± 0.040 |
| M_{bol} (mag) | 2.50 ± 0.10 | 2.40 ± 0.11 |
| Interstellar reddening $E(B-V)$ (mag) | 0.05 ± 0.02 | |
| Distance (pc) | 176.0 ± 3.7 | |

Comparison with theoretical models

We compared the properties of RZ Cha to the predictions of the PARSEC 1.2.5 theoretical stellar-evolutionary models^{50,49} in the mass–radius and mass– T_{eff} diagrams. We obtained an acceptable fit for a metal abundance of $Z = 0.017$ and an age of 2.35 ± 0.10 Gyr, in the sense that the theoretical isochrones passed within 1σ of the measured properties. A slightly lower metal abundance of $Z = 0.014$ gave a better fit for an age of 2.20 ± 0.10 Gyr, in that the T_{eff} values were matched almost exactly rather than at the 1σ lower error bar.

Jørgensen & Gyldenkerne¹¹ found that the components of RZ Cha have evolved beyond the main sequence by comparing their properties with the theoretical models of Hejlesen^{51,52}. AG175 confirmed the conclusion that both component stars were in the subgiant phase. We investigated this by plotting a Hertzsprung–Russell diagram (Fig. 5) with the stars and PARSEC evolutionary tracks for a range of masses. This clearly shows that both components are within the main-sequence band, and that an age of 2.05 Gyr is the best match. We find a younger age than in the previous paragraph because we have striven to match T_{eff} and luminosity rather than mass, radius, and T_{eff} . That we find the components to be main-sequence stars rather than subgiants is due to the inclusion of convective-core overshooting in more modern theoretical models, which causes the main-sequence band to extend to higher luminosities^{53,54}.

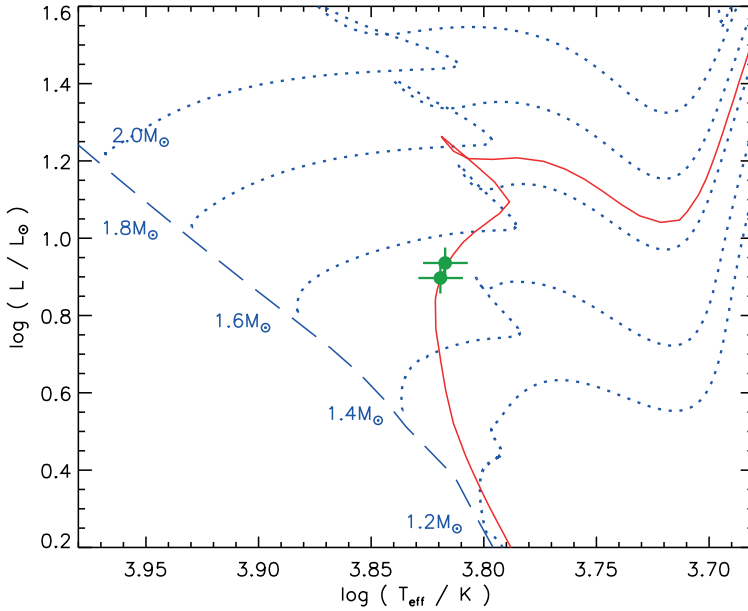


FIG. 5

Hertzsprung–Russell diagram for the components of RZ Cha (filled green circles) and the predictions of the PARSEC 1:2S models⁴⁹ for selected masses (dotted blue lines with masses labelled) and the zero-age main sequence (dashed blue line), for a metal abundance of $Z = 0.017$. The isochrone for an age of 2.05 Gyr is shown with a solid red line.

Summary and conclusions

RZ Cha is a dEB containing two F5 stars in a circular orbit of period 2.832 d. We used light-curves from the *TESS* mission and spectroscopic orbits from *Gaia* DR3 to determine the masses and radii of the component stars. With the addition of a published T_{eff} measurement and surface-brightness calibrations we determined their luminosities and the distance to the system. The distance we find, 176.7 ± 3.7 pc, agrees with the value of 174.2 ± 0.6 pc from *Gaia* DR3. The two stars are very similar, having almost identical masses and T_{eff} values, but star B is larger and thus brighter. We find a mass ratio below unity, in modest disagreement with published values from ground-based spectroscopy, and this result can be checked in the near future when the *Gaia* RVs are published.

Both components are in the upper part of the main-sequence band in the Hertzsprung–Russell diagram, in contrast to previous claims that they have evolved beyond the main-sequence stage. We find acceptable matches to the masses, radii, T_{eff} values, and luminosities of the stars for a metal abundance around or slightly below solar, and an age in the region of 2.3 Gyr.

Both components of RZ Cha are within the region of the Hertzsprung–Russell diagram where g-mode pulsations can be found^{45,56}, and relatively few g-mode pulsators in dEBs are known^{57,58}. We therefore checked the *TESS* light-

curves for signs of pulsations by fitting them with JKTEBOP to remove the signals of binarity, then calculating periodograms using the PERIODO4 code⁵⁹. This was done for *TESS* sectors 11–13, 38 and 39, and 65 and 66. Several possible low-amplitude pulsation frequencies below 3 d^{-1} were found, but none were consistently present in the three periodograms. A periodogram at the Nyquist frequency of 360 d^{-1} was calculated for sectors 65 and 66, and showed no significant power beyond 3 d^{-1} . We therefore conclude that there is no evidence for pulsations in RZ Cha.

Acknowledgements

We are grateful to Dr. Pierre Maxted for calculating which star is the primary component in the *Gaia* spectroscopic orbit, and to the anonymous referee for a positive and prompt report. This paper includes data collected by the *TESS* mission and obtained from the MAST data archive at the Space Telescope Science Institute (STScI). Funding for the *TESS* mission is provided by the NASA's Science Mission Directorate. STScI is operated by the Association of Universities for Research in Astronomy, Inc., under NASA contract NAS 5–26555. This work has made use of data from the European Space Agency (ESA) mission *Gaia*^{*}, processed by the *Gaia* Data Processing and Analysis Consortium (DPAC[†]). Funding for the DPAC has been provided by national institutions, in particular the institutions participating in the *Gaia* Multilateral Agreement. The following resources were used in the course of this work: the NASA Astrophysics Data System; the *Simbad* database operated at CDS, Strasbourg, France; and the arXiv scientific-paper preprint service operated by Cornell University.

References

- (1) J. Southworth, *The Observatory*, **140**, 247, 2020.
- (2) J. Andersen, *A&ARv*, **3**, 91, 1991.
- (3) G. Torres, J. Andersen & A. Giménez, *A&ARv*, **18**, 67, 2010.
- (4) P. F. L. Maxted *et al.*, *MNRAS*, **498**, 332, 2020.
- (5) W. J. Borucki, *Reports on Progress in Physics*, **79**, 036901, 2016.
- (6) G. R. Ricker *et al.*, *Journal of Astronomical Telescopes, Instruments, and Systems*, **1**, 014003, 2015.
- (7) J. Southworth, *Universe*, **7**, 369, 2021.
- (8) W. Strohmeier, R. Knigge & H. Ott, *IBVS*, **66**, 1, 1964.
- (9) D. M. Popper, *AJ*, **71**, 175, 1966.
- (10) E. H. Geyer & R. Knigge, *IBVS*, **941**, 1, 1974.
- (11) H. E. Jørgensen & K. Gyldenkerne, *A&A*, **44**, 343, 1975.
- (12) H. N. Russell & J. E. Merrill, *The determination of the elements of eclipsing binaries* (Contributions from the Princeton University Observatory, Princeton), 1952.
- (13) K. Gyldenkerne, H. E. Jørgensen & E. Carstensen, *A&A*, **42**, 303, 1975.
- (14) J. Andersen, H. Gjerløff & M. Imbert, *A&A*, **44**, 349, 1975.
- (15) G. Giuricin *et al.*, *A&A*, **85**, 259, 1980.
- (16) D. B. Wood, *PASP*, **85**, 253, 1973.
- (17) D. Graczyk *et al.*, *Apf*, **837**, 7, 2017.
- (18) E. Høg *et al.*, *A&A*, **355**, L27, 2000.
- (19) R. M. Cutri *et al.*, *2MASS All Sky Catalogue of Point Sources* (The IRSA 2MASS All-Sky Point Source Catalogue, NASA/IPAC Infrared Science Archive, Caltech, US), 2003.
- (20) *Gaia* Collaboration, *A&A*, **674**, A1, 2023.
- (21) A. J. Cannon & E. C. Pickering, *Annals of Harvard College Observatory*, **94**, 1, 1919.
- (22) *Gaia* Collaboration, *A&A*, **649**, A1, 2021.
- (23) K. G. Stassun *et al.*, *AJ*, **158**, 138, 2019.
- (24) J. N. Winn, chapter in the *Handbook of Exoplanets*, arXiv:2410.12905, 2024.

* <https://www.cosmos.esa.int/Gaia>

† <https://www.cosmos.esa.int/web/Gaia/dpac/consortium>

- (25) Lightkurve Collaboration, ‘Lightkurve: Kepler and TESS time series analysis in Python’, Astrophysics Source Code Library, 2018.
- (26) J. M. Jenkins *et al.*, in *Proc. SPIE*, 2016, *Society of Photo-Optical Instrumentation Engineers (SPIE) Conference Series*, vol. 9913, p. 99133E.
- (27) J. Southworth, P. F. L. Maxted & B. Smalley, *MNRAS*, **351**, 1277, 2004.
- (28) J. Southworth, *A&A*, **557**, A119, 2013.
- (29) D. Hestroffer, *A&A*, **327**, 199, 1997.
- (30) P. F. L. Maxted, *A&A*, **616**, A39, 2018.
- (31) J. Southworth, *The Observatory*, **143**, 71, 2023.
- (32) A. Claret & J. Southworth, *A&A*, **664**, A128, 2022.
- (33) A. Claret & J. Southworth, *A&A*, **674**, A63, 2023.
- (34) J. Southworth, *MNRAS*, **386**, 1644, 2008.
- (35) A. Mallama, *PASP*, **93**, 774, 1981.
- (36) J. M. Kreiner, C.-H. Kim & I.-S. Nha, *An atlas of O-C diagrams of eclipsing binary stars*, 2001.
- (37) M. Cropper *et al.*, *A&A*, **616**, A5, 2018.
- (38) Gaia Collaboration, *A&A*, **674**, A34, 2023.
- (39) L. B. Lucy & M. A. Sweeney, *AJ*, **76**, 544, 1971.
- (40) D. Bashi *et al.*, *MNRAS*, **517**, 3888, 2022.
- (41) A. Tokovinin, *AJ*, **165**, 220, 2023.
- (42) M. L. Marcussen & S. H. Albrecht, *AJ*, **165**, 266, 2023.
- (43) J. Southworth, *The Observatory*, **143**, 165, 2023.
- (44) J. Southworth, *The Observatory*, **144**, 242, 2024.
- (45) A. Prša *et al.*, *AJ*, **152**, 41, 2016.
- (46) J. Southworth, P. F. L. Maxted & B. Smalley, *A&A*, **429**, 645, 2005.
- (47) J. Southworth, *The Observatory*, **144**, 181, 2024.
- (48) P. Kervella *et al.*, *A&A*, **426**, 297, 2004.
- (49) Y. Chen *et al.*, *MNRAS*, **444**, 2525, 2014.
- (50) A. Bressan *et al.*, *MNRAS*, **427**, 127, 2012.
- (51) P. M. Hejlesen, *A&A*, **84**, 135, 1980.
- (52) P. M. Hejlesen, *A&AS*, **39**, 347, 1980.
- (53) A. Maeder & G. Meynet, *A&A*, **210**, 155, 1989.
- (54) R. B. Stothers, *ApJ*, **383**, 820, 1991.
- (55) L. A. Balona & D. Ozuyar, *MNRAS*, **493**, 5871, 2020.
- (56) J. S. G. Mombarg *et al.*, *A&A*, **691**, A131, 2024.
- (57) P. Gaulme & J. A. Guzik, *A&A*, **630**, A106, 2019.
- (58) J. Southworth & T. Van Reeth, *MNRAS*, **515**, 2755, 2022.
- (59) P. Lenz & M. Breger, *Communications in Asteroseismology*, **146**, 53, 2005.

REVIEWS

Attention is Discovery. The Life and Legacy of Astronomer Henrietta Leavitt, by Anna Von Mertens (MIT Press), 2024. Pp. 256, 26 × 21 cm. Price £32/\$34.95 (hardbound; ISBN 978 0 262 04938 2).

This is a biography with a difference: a life in science seen through the eyes of an artist. Henrietta Swan Leavitt is internationally known as the discoverer of what has long been known as the period–luminosity relation for Cepheid variables (officially renamed by the IAU in 2008 as Leavitt’s Law), but this book makes it very clear what a laborious task it was to discover it — first noticed and published in 1908 (as a single sentence in a paper recording details of 1177 variables, with 16 variables in Table VI: “It is worthy of notice that in Table VI the brighter variables have the longer periods”), and confirmed four years later after more detailed study with more Cepheids.

In our day, it is hard to remember the revolution caused by the replacement of photographic records by digital ones recorded by CCDs. Miss Leavitt was one of the famous women ‘computers’ at Harvard College Observatory in the early 1900s who meticulously studied and recorded information contained on